

# Generalized Fourier’s law in mesoscopic systems

Luciano C. Lapas<sup>✉\*</sup>

*Latin American Institute of Life and Natural Sciences,  
Universidade Federal da Integração Latino-Americana, Av. Tancredo Neves,  
6731, Bloco 6, Espaço 3, Sala 5, Foz do Iguaçu, 85867-970, PR, Brazil.*

(Dated: June 24, 2026)

Fourier’s law fails when the mean free path of the energy carriers becomes comparable to the length and time scales over which the temperature field varies. We derive a thermodynamically consistent generalization in which the conductivity is promoted to a nonlocal memory operator  $\kappa_{\text{eff}}(\mathbf{k}, \omega)$ , obtained by combining mesoscopic nonequilibrium thermodynamics with the Mori–Kubo–Zwanzig projection-operator formalism. The Onsager kernel decomposes exactly into a tensor sum over vibrational normal modes weighted by their Bose heat capacities and relaxation functions, and satisfies the second law by construction. Two consequences follow. First, because the modal weights carry the directional group velocity, the kernel is anisotropic, so a nominally isotropic crystal exhibits direction-dependent apparent conductivities  $\Lambda_z \neq \Lambda_r$ . Second, in a pump–probe experiment the modulation frequency does not introduce temporal memory but sets the probed wavevector through the thermal penetration depth, so the suppression of the apparent conductivity measured by time-domain thermoreflectance on Si, Ge and  $\text{Si}_{1-x}\text{Ge}_x$  is a spatial-nonlocality effect set by a sub-micron carrier mean free path. Fitting the data of Wilson and Cahill yields nonlocality lengths of 0.25–0.4  $\mu\text{m}$  consistent with the mean-free-path spectra of these crystals. The framework supplies a thermodynamic foundation for the two-channel ballistic/diffusive picture of nondiffusive heat transport.

*Introduction.*—The classical theory of heat conduction rests on Fourier’s law,

$$\mathbf{J}_q = -\kappa \nabla T, \quad (1)$$

relating the heat flux  $\mathbf{J}_q$  to the local temperature gradient through a scalar conductivity  $\kappa$ . Equation (1) is accurate whenever the carrier mean free path (MFP)  $\ell_c$  is far shorter than the experimental length scale  $L_{\text{exp}}$ , i.e. in the diffusive regime where the Knudsen number  $\text{Kn} \equiv \ell_c/L_{\text{exp}} \ll 1$  and carriers (e.g., phonons in dielectrics and most semiconductors, electrons in metals [1, 2]) relax to local equilibrium much faster than the macroscopic field evolves. Local energy conservation then yields the diffusion equation  $\partial_t T = a \nabla^2 T$  [3, 4], and a localized pulse spreads into a Gaussian profile of width  $\ell(t) \sim 2\sqrt{at}$ . This description breaks down when  $L_{\text{exp}}$  is no longer large compared with the longest active MFP, as in nanostructures [5], colloids [6], and biological organelles [7], where  $\text{Kn} \gtrsim \mathcal{O}(1)$  marks the onset of nonlocal, partially ballistic transport [2, 8]. Quantitative evidence is now abundant: quasiballistic transport and size-dependent effective conductivity in silicon membranes [9]; the anisotropic failure of Fourier’s law in time-domain thermoreflectance (TDTR) on Si and SiGe [10]; and non-Gaussian temperature profiles in translucent polymers and glasses, where internal infrared radiation provides an additional transport channel with millimetre-scale effective MFPs [11].

These breakdowns are not all of the same kind, and a useful theory must distinguish them. The general constitutive response is nonlocal in both time and space, but a given experiment probes one axis preferentially. In TDTR the relevant timescale  $1/f$  is far longer than

carrier lifetimes, so temporal memory is negligible and the modulation frequency  $f$  acts only by fixing a spatial scale, the thermal penetration depth  $d_p = \sqrt{\kappa_{\text{ref}}/\pi C f}$ , with  $C$  the volumetric heat capacity [10]; here  $\kappa_{\text{ref}}$  denotes a fixed diffusive reference conductivity used to define an effective thermal length scale (we take  $\kappa_{\text{ref}} = \kappa_{\text{bulk}}$  below to avoid circularity when  $\Lambda_A$  depends on  $f$ ); the same holds for the macroscale radiative anomaly of Ref. [11]. Temporal memory dominates instead in second-sound and transient-grating geometries [12]. The TDTR breakdown is moreover *anisotropic*: beam-offset measurements on nominally isotropic Si return distinct through-plane and in-plane conductivities,  $\Lambda_z \approx 140$  and  $\Lambda_r \approx 80 \text{ W m}^{-1} \text{ K}^{-1}$  [10, 13], and it is interface mediated, requiring a nonequilibrium resistance beyond a local boundary conductance [10]. Following Wilson and Cahill, we use  $\Lambda_A$ ,  $\Lambda_z$ , and  $\Lambda_r$  to denote *apparent* conductivities extracted by fitting TDTR data with local diffusive models, while  $\kappa_{\text{bulk}}$  denotes the intrinsic bulk conductivity in the Fourier limit. A compact constitutive law that captures these features while remaining thermodynamically consistent is still lacking. The phonon Boltzmann transport equation reproduces the kinetics [14, 15] but is computationally heavy; phenomenological extensions such as the Cattaneo-Vernotte equation [16, 17] restore finite speeds but lack a general entropy-production principle.

In this Letter we construct the missing relation. Combining mesoscopic nonequilibrium thermodynamics (MNET) [18–20] with the Mori–Kubo–Zwanzig projection-operator formalism [21–24] promotes the conductivity to a nonlocal memory operator  $\kappa_{\text{eff}}(\mathbf{k}, \omega)$  whose Onsager kernel decomposes into vibrational nor-

mal modes weighted by Bose heat capacities. We show that this single kernel (i) produces apparent anisotropy  $\Lambda_z \neq \Lambda_r$  as a consequence of the directional modal weights, (ii) reproduces the TDTR conductivities of Si, Ge and  $\text{Si}_{1-x}\text{Ge}_x$  as a spatial-nonlocality effect set by  $d_p(f)$  and governed by a single material length, and (iii) supplies a microscopic, entropy-producing foundation for the two-channel ballistic/diffusive description of nondiffusive transport [10, 12, 25].

*Generalized constitutive relation.*—We extend the validity of the Gibbs equation to internal degrees of freedom  $\mathbf{\Gamma} = (\mathbf{p}, \mathbf{r})$  that have not yet relaxed to local equilibrium. For a phase-space density  $\rho(\mathbf{\Gamma}, t)$  of heat carriers, the entropy production rate is  $\sigma = -\int \mathbf{J}_{\mathbf{\Gamma}} \cdot \nabla_{\mathbf{\Gamma}}(\mu/T) d\mathbf{\Gamma} \geq 0$ , with  $\mu(\mathbf{\Gamma}, t)$  a nonequilibrium chemical potential [19, 20]. Even in steady state, bosonic carriers can acquire a nonzero effective chemical potential, as in near-field photonic cooling [26] and nonequilibrium Casimir experiments [27].

Postulating a causal linear response in phase space consistent with  $\sigma \geq 0$ , and coarse-graining onto the energy-density field, yields a generalized constitutive law for the macroscopic heat flux (see Supplemental Material [28]),

$$\mathbf{J}_q(\mathbf{r}, t) = \int_{-\infty}^t dt' \int d\mathbf{r}' \mathbf{L}_{qq}(\mathbf{r}, \mathbf{r}', t - t') \nabla_{\mathbf{r}'} \left[ \frac{1}{T(\mathbf{r}', t')} \right]. \quad (2)$$

The spatiotemporal kernel  $\mathbf{L}_{qq}$  is not *ad hoc*: it arises from the projection of phase-space correlations connecting transport at  $\mathbf{r}'$  to  $\mathbf{r}$  through carrier propagation and scattering, and its symmetric part is positive semidefinite, guaranteeing  $\sigma \geq 0$  [28]. Linearizing about a reference  $T_0$  via  $\nabla(1/T) \simeq -T_0^{-2} \nabla \delta T$  and Fourier transforming in space and time recasts Eq. (2) as a generalized Fourier law,

$$\mathbf{J}_q(\mathbf{k}, \omega) = -i \boldsymbol{\kappa}_{\text{eff}}(\mathbf{k}, \omega) \cdot \mathbf{k} \delta T(\mathbf{k}, \omega), \quad (3)$$

with  $\boldsymbol{\kappa}_{\text{eff}}(\mathbf{k}, \omega) \equiv \tilde{\mathbf{L}}_{qq}(\mathbf{k}, \omega)/T_0^2$  the generalized conductivity tensor. The classical law, Eq. (1), is recovered strictly in the hydrodynamic limit  $\mathbf{k} \rightarrow 0$ ,  $\omega \rightarrow 0$ , where the kernel reduces to a Dirac delta in space and time and  $\boldsymbol{\kappa}_{\text{eff}} \rightarrow \boldsymbol{\kappa} \mathbf{1}$ . In TDTR (linear, time-invariant regime), the measured surface response can be written as a Hankel-space integral over radial spatial frequencies  $k$ , weighted by the pump/probe beam profiles [13]; thus the experiment is, strictly, sensitive to a *distribution* of spatial frequencies rather than a single  $k$ . Crucially, a pump–probe experiment is nevertheless well summarized by effective length scales that set the dominant gradients: through-plane,  $d_p(f) = \sqrt{\kappa_{\text{ref}}/\pi C f}$  and an associated effective  $k_z(f) \sim d_p^{-1}(f)$ ; and in-plane, the spot size  $w_0$  and an associated effective  $k_r \sim w_0^{-1}$ . The apparent conductivities extracted from fitting a local diffusive TDTR model are therefore directional *proxies* for  $\boldsymbol{\kappa}_{\text{eff}}(\mathbf{k})$  and diagnose spatial nonlocality rather than temporal memory [10].

*Modal kernel and anisotropy.*—To ground the kernel microscopically we project the Liouville evolution of  $\mathbf{\Gamma}$  onto a column vector  $\mathbf{A}(t)$  of slow variables. The Mori–Kubo–Zwanzig identity yields the exact generalized Langevin equation (GLE) [28],

$$\frac{d\mathbf{A}(t)}{dt} = i\boldsymbol{\Omega} \mathbf{A}(t) - \int_0^t d\tau \boldsymbol{\Phi}(\tau) \mathbf{A}(t - \tau) + \mathbf{F}(t), \quad (4)$$

with  $\boldsymbol{\Omega}$  the reversible frequency matrix,  $\mathbf{F}(t)$  the projected stochastic force, and the memory kernel obeying the fluctuation–dissipation theorem  $\boldsymbol{\Phi}(\tau) = \langle \mathbf{F}(\tau) \mathbf{F}^T(0) \rangle \mathbf{C}^{-1}$ ,  $\mathbf{C} \equiv \langle \mathbf{A} \mathbf{A}^T \rangle$ . The normalized propagator  $\mathbf{R}(t) = \mathbf{C}(t) \mathbf{C}^{-1}$  has Laplace transform  $\tilde{\mathbf{R}}(z) = [z\mathbf{1} + \tilde{\boldsymbol{\Phi}}(z)]^{-1}$ , whose poles set the mesoscopic timescales.

Choosing the components of  $\mathbf{A}$  as the modal energy fluctuations  $A_\mu(t) = \delta E_\mu(t) = \varepsilon_\mu [n_\mu(t) - n_\mu^{\text{eq}}]$  of the vibrational eigenmodes  $\phi_\mu(\mathbf{r})$  of the confined medium (with  $\varepsilon_\mu = \hbar\omega_\mu$ ), the heat flux separates into geometry and dynamics,  $\mathbf{J}_q(\mathbf{r}, t) = \sum_\mu \boldsymbol{\Psi}_\mu(\mathbf{r}) A_\mu(t)$ , with the *vectorial* mode flux functions

$$\boldsymbol{\Psi}_\mu(\mathbf{r}) = \mathbf{v}_\mu(\mathbf{r}) |\phi_\mu(\mathbf{r})|^2 \quad (5)$$

carrying the directional group velocity  $\mathbf{v}_\mu$ . The Onsager kernel then follows in closed, tensor form [28],

$$L_{qq}^{ij}(\mathbf{r}, \mathbf{r}', t) = \sum_{\mu, \nu} \Psi_\mu^i(\mathbf{r}) \Psi_\nu^j(\mathbf{r}') R_{\mu\nu}(t) c_{\text{ph}}(\omega_\nu, T), \quad (6)$$

where the classical variance is replaced by the spectral (Bose) heat capacity

$$c_{\text{ph}}(\omega, T) = k_B \left( \frac{\hbar\omega}{2k_B T} \right)^2 \text{csch}^2 \left( \frac{\hbar\omega}{2k_B T} \right). \quad (7)$$

Equation (6) is the central structural result. Spatial nonlocality is carried by the mode overlap  $\Psi_\mu^i(\mathbf{r}) \Psi_\nu^j(\mathbf{r}')$ ; temporal memory resides in  $R_{\mu\nu}(t)$ ; and the quantum weight  $c_{\text{ph}}(\omega_\nu, T)$  “freezes out” high-frequency modes for  $k_B T \ll \hbar\omega_\nu$ , correcting the systematic overestimate of heat flow by classical models below the Debye temperature [8, 29]. Distinct carrier families (acoustic and optical phonons, or internal radiation in translucent solids [11]) enter additively through disjoint mode sectors.

The tensor structure of Eq. (6) has an immediate, testable consequence. Fourier transforming in space and time, the diagonal blocks of the conductivity read

$$\kappa_{\text{eff}}^{ii}(\mathbf{k}, \omega) = \frac{1}{T_0^2} \sum_{\mu, \nu} \tilde{\Psi}_\mu^i(\mathbf{k}) \tilde{\Psi}_\nu^i(-\mathbf{k}) \tilde{R}_{\mu\nu}(\omega) c_{\text{ph}}(\omega_\nu, T), \quad (8)$$

where the overlap  $\tilde{\Psi}_\mu^i(\mathbf{k}) \tilde{\Psi}_\nu^i(-\mathbf{k})$  is maximal at  $\mathbf{k} \rightarrow 0$  (extended modes) and is cut off for  $|\mathbf{k}| \gtrsim \ell^{-1}$ , so each block decreases monotonically with  $|\mathbf{k}|$ . Because  $\boldsymbol{\Psi}_\mu$  points along the mode group velocity, the through- and in-plane blocks generally differ; evaluated at the

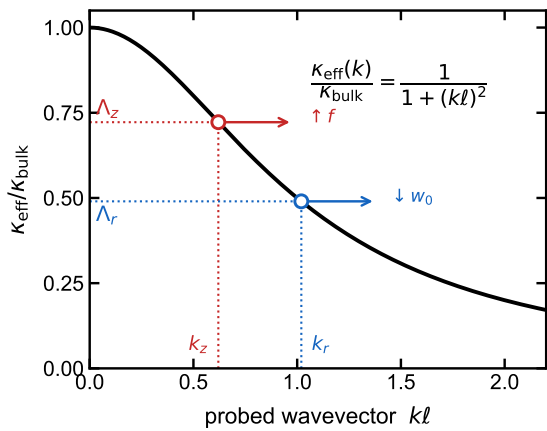


FIG. 1. Anisotropy from a single nonlocal kernel. The effective conductivity falls with the probed wavevector,  $\kappa_{\text{eff}}(k)/\kappa_{\text{bulk}} = [1 + (k\ell)^2]^{-1}$ . A TDTR experiment samples the through-plane direction at  $k_z \sim d_p^{-1}(f)$  and the in-plane direction at  $k_r \sim w_0^{-1}$ , so a nominally isotropic crystal yields  $\Lambda_z \neq \Lambda_r$ . Increasing the modulation frequency  $f$  (decreasing the spot size  $w_0$ ) shifts  $k_z$  ( $k_r$ ) outward, selectively suppressing each channel.

direction-dependent wavevectors of a TDTR experiment,  $k_z \simeq d_p^{-1}(f) = \sqrt{\pi C f / \kappa_{\text{ref}}}$  and  $k_r \simeq w_0^{-1}$ , this yields

$$\Lambda_z = \kappa_{\text{eff}}^{zz}(k_z \sim d_p^{-1}) \neq \Lambda_r = \kappa_{\text{eff}}^{rr}(k_r \sim w_0^{-1}), \quad (9)$$

with the more strongly sampled direction the more suppressed (Fig. 1). For Si at  $w_0 \approx 1 \mu\text{m}$  and  $f = 9.8 \text{ MHz}$ , with  $\kappa_{\text{ref}} \approx 142 \text{ W m}^{-1} \text{ K}^{-1}$  (taken as the bulk value) and  $C \approx 1.6 \times 10^6 \text{ J m}^{-3} \text{ K}^{-1}$ , one finds  $d_p \approx 1.7 \mu\text{m}$ , hence  $k_z \approx 0.6 < k_r \approx 1.0 \mu\text{m}^{-1}$  and  $\Lambda_r < \Lambda_z$ , in qualitative agreement with the beam-offset observation  $\Lambda_z \approx 140$ ,  $\Lambda_r \approx 80 \text{ W m}^{-1} \text{ K}^{-1}$  [10, 13]: a nominally isotropic kernel produces apparent anisotropy purely through direction-dependent sampling. Raising  $f$  shifts  $k_z$  outward and suppresses the through-plane channel; shrinking  $w_0$  shifts  $k_r$  outward and suppresses the in-plane channel, reproducing the experimentally observed selectivity of the two knobs [10]. A fully quantitative account of the  $(\Lambda_z, \Lambda_r)$  pair, which also involves the breakdown of Fourier's law near temperature-profile extrema [10], requires the full tensor  $\kappa_{\text{eff}}^{ij}(\mathbf{k})$  together with the multilayer thermal forward model; here we establish the mechanism and turn to the quantitative through-plane data, where the mapping is direct.

*Limiting cases.*—The low-frequency structure of  $\tilde{\Phi}(z)$  classifies the transport regimes [28, 30–32]: a spectral density  $S(\omega) \propto \omega^s$  gives  $\tilde{\Phi}(z) \sim z^{s-1}$ , with the Ohmic case  $s = 1$  producing finite friction, exponential relaxation, and the generalized Einstein relation  $\mathbf{L}_{\text{Onsager}} = (k_B T)^{-1} [\gamma^*]^{-1} \mathbf{C}_0$ , hence Fourier's law; sub- and super-Ohmic spectra give sub- and superdiffusion, and  $s = 2$  the ballistic saturation  $\mathbf{R}(\infty) \neq \mathbf{0}$  [33, 34]. The two textbook limits follow as special cases. A Markovian

kernel  $\Phi(t) \approx 2\gamma \delta(t)$  gives Fourier's law; a single inertial pole,  $\tilde{\Phi}(z) \approx \tau_q^{-1} \mathbf{1}$ , gives the Cattaneo–Vernotte equation  $\tau_q \partial_t \mathbf{J}_q + \mathbf{J}_q = -\kappa \nabla T$ , with  $\tau_q$  now identified as the inertial relaxation time of the flux. We stress that this temporal-memory limit is relevant to second-sound propagation, where  $\omega \tau_q \sim 1$ ; by contrast, transient-grating [12] and pump-probe geometries operate at  $1/f \gg \tau_q$  and are governed by the spatial nonlocality analyzed below, in which the modulation frequency sets a probed wavevector rather than a memory time.

*Spatial nonlocality and the TDTR data.*—In TDTR the modulation frequency sets the through-plane length scale through  $d_p = \sqrt{\kappa_{\text{ref}} / \pi C f}$ , so the probe samples the conductivity at  $k_z \simeq d_p^{-1}$ . Because TDTR observables are weighted integrals over spatial frequencies [13], we interpret  $k_z \simeq d_p^{-1}$  as an effective through-plane wavevector associated with the dominant gradients in a diffusive reference model. To lowest order in gradients the isotropic nonlocal conductivity is well captured by a minimal one-length ansatz, a Lorentzian in wavevector,

$$\kappa_{\text{eff}}(k) = \frac{\kappa_{\text{bulk}}}{1 + (k\ell)^2}, \quad (10)$$

which is the [0/1] Padé closure consistent with the long-wavelength expansion of a finite-range spatial kernel (see Supplemental Material, Sec. SIV.A). Equation (10) is consistent with long-wavelength gradient expansions and widely used nonlocal forms (e.g. Guyer–Krumhansl/Mahan–Claro-type parametrizations) [35, 36]; its derivation from an entropy-producing GLE, the explicit Bose weighting  $c_{\text{ph}}$ , and the modal reading of the interface (below) are what distinguish the present framework from earlier nonlocal and quasiballistic BTE treatments [15, 37, 38]. Evaluated at  $k_z = d_p^{-1}$  this gives a frequency-resolved apparent conductivity (apparent in the sense of Wilson and Cahill, i.e. extracted by fitting a local diffusive TDTR model [10])

$$\Lambda_A(f) = \frac{\kappa_{\text{bulk}}}{1 + f/f^*}, \quad f^* = \frac{\kappa_{\text{ref}}}{\pi C \ell^2}, \quad (11)$$

controlled by a single material length  $\ell$  rather than a fitted relaxation time. The crossover frequency  $f^*$  is large (response flat) when  $\ell$  is short, and small (early roll-off) when  $\ell$  is long.

Figure 2 compares Eq. (11) with the apparent conductivities of Wilson and Cahill [10] over  $f = 1\text{--}20 \text{ MHz}$ ; a two-parameter fit  $(\kappa_{\text{bulk}}, \ell)$  per material reproduces every data set within experimental error ( $\chi_\nu^2 < 1$ ). Pure Si and boron-doped Si:B remain flat: their high conductivity keeps  $d_p \gg \ell$  throughout the band, so  $\ell$  is unresolved (consistent with the sub-micron values below). The SiGe alloys and Ge roll off and return well-constrained, sub-micron nonlocality lengths,  $\ell_{\text{Ge}} = 0.41 \pm 0.08$ ,  $\ell_{\text{Si}_{0.99}\text{Ge}_{0.01}} = 0.34 \pm 0.07$ , and  $\ell_{\text{Si}_{0.2}\text{Ge}_{0.8}} = 0.25 \pm 0.03 \mu\text{m}$  (for the alloys the fitted  $\kappa_{\text{bulk}}$  lies somewhat below the literature bulk value, absorbing the suppression already present at the lowest  $f$ ). Two features

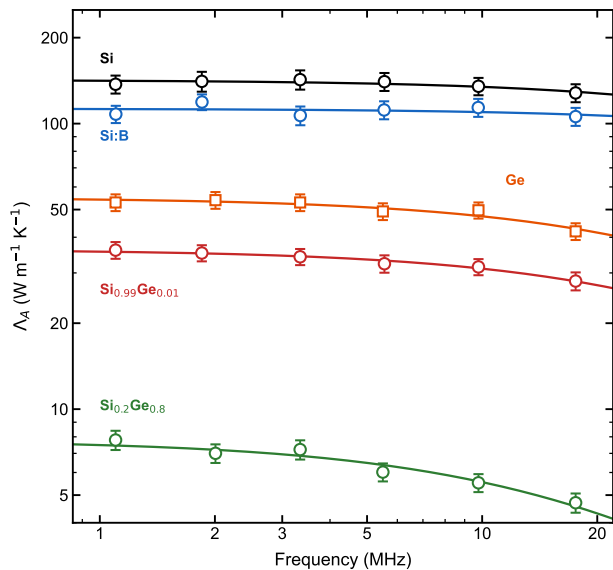


FIG. 2. Apparent thermal conductivity  $\Lambda_A$  versus modulation frequency: the spatial-nonlocality model, Eq. (11) (solid lines), against TDTR data of Wilson and Cahill [10] (symbols, with error bars; digitized from their Fig. 3a at  $w_0 = 10 \mu\text{m}$ ). Fourier’s law predicts a constant  $\Lambda_A$ ; Si and Si:B stay flat while Ge and the SiGe alloys are suppressed at high  $f$ , where the shrinking penetration depth  $d_p(f)$  probes a larger wavevector. Solid lines are two-parameter fits of Eq. (11); the resolved nonlocality lengths are  $\ell = 0.41, 0.34$  and  $0.25 \mu\text{m}$  for Ge,  $\text{Si}_{0.99}\text{Ge}_{0.01}$  and  $\text{Si}_{0.2}\text{Ge}_{0.8}$ , respectively.

are transparent in Eq. (6). First, alloy mass-disorder scattering [39] shortens the carrier mean free path, so  $\ell$  decreases as Ge is alloyed into Si, ordered Ge being the longest. Second, the high-frequency suppression nonetheless deepens with alloying because the low alloy conductivity shrinks  $d_p$  and pushes the probed wavevector  $k_z = d_p^{-1}$  further into the nonlocal regime. The fitted lengths fall within the sub-micron MFP range that dominates the conductivity accumulation function  $\alpha(L)$  of these crystals [10, 15], a length scale set by the dominant heat-carrying modes rather than an independently adjusted parameter.

*Role of the interface.*—The same modal picture clarifies why a local boundary conductance is insufficient [10]. Near a metal/sample boundary the reflected and transmitted modes truncate the overlap  $\Psi_\mu^i(\mathbf{r})\Psi_\nu^j(\mathbf{r}')$  within a layer of thickness set by the MFP, leaving residual off-diagonal correlations  $R_{\mu\nu}$  ( $\mu \neq \nu$ ) that do not relax to a single local temperature. In the language of Eq. (6), the high- and low-wavevector sectors are driven out of mutual equilibrium over a finite length, which is precisely the interfacial nonequilibrium resistance inferred phenomenologically from the frequency dependence of the apparent interface conductance in SiGe alloys [10]. The kernel thus places the diffusive reservoir and the nonlocal ballistic channel of the two-fluid description [12, 25] on a

common, entropy-producing footing, rather than positioning them separately.

*Conclusion.*—We have derived a thermodynamically consistent generalization of Fourier’s law in which the conductivity is a nonlocal memory operator  $\kappa_{\text{eff}}(\mathbf{k}, \omega)$ , whose Onsager kernel decomposes exactly into vibrational normal modes weighted by Bose heat capacities and relaxation functions [Eq. (6)]. The tensor structure of the modal weights makes the kernel anisotropic, so that direction-dependent sampling of an otherwise isotropic kernel yields apparent anisotropy  $\Lambda_z \neq \Lambda_r$  in a nominally isotropic crystal; the recognition that TDTR samples  $\kappa_{\text{eff}}$  at a frequency-set wavevector  $k_z \sim d_p^{-1}$  (in an effective sense, since the signal is a weighted integral over spatial frequencies [13]) recasts the measured suppression in Si, Ge and SiGe as spatial nonlocality set by a sub-micron mean free path, extracted here as  $\ell \simeq 0.25\text{--}0.4 \mu\text{m}$ ; and the truncation of modal overlaps at a boundary provides a microscopic origin for the interfacial nonequilibrium resistance. Together these results furnish the thermodynamic and microscopic foundation that the phenomenological two-channel ballistic/diffusive picture has lacked [10, 12, 25], with the falsifiable prediction that the nonlocality length should coincide with the MFP scale of the conductivity accumulation function. Because the kernel is expressed through equilibrium correlation functions and modal heat capacities, the framework connects experimental observables to microscopic parameters without ad hoc extensions, and applies directly to nanowires, superlattices and quantum dots, to the temperature dependence of nondiffusive transport through  $c_{\text{ph}}(\omega, T)$ , and, by extension to electronic variables, to thermoelectric and active quantum devices [40].

The author gratefully acknowledges the financial support by National Institute of Science and Technology in Innovative Research in Health Sciences – from Nanotechnology to Artificial Intelligence (INCT PICS) sponsored by Brazil’s National Council for Scientific and Technological Development (CNPq), grant no. 408417/2024-2.

\* luciano.lapas@unila.edu.br

- [1] G. Chen, *Nanoscale Energy Transport and Conversion: A Parallel Treatment of Electrons, Molecules, Phonons, and Photons* (Oxford University Press, New York, 2005).
- [2] J.-J. Greffet, *Electrons and Phonons*, in *Microscale and Nanoscale Heat Transfer*, edited by S. Volz (Springer Berlin Heidelberg, Berlin, Heidelberg, 2007) pp. 37–54.
- [3] J. B. J. Fourier, *Théorie analytique de la chaleur* (Didot, Paris, 1822).
- [4] J.-J. Greffet, *Laws of Macroscopic Heat Transfer and Their Limits*, in *Microscale and Nanoscale Heat Transfer*, edited by S. Volz (Springer Berlin Heidelberg, Berlin, Heidelberg, 2007) pp. 1–13.
- [5] D. Bimberg, M. Grundmann, and N. N. Ledentsov, *Quantum dot heterostructures* (John Wiley & Sons,

- Chichester, 1999).
- [6] B. J. Berne and R. Pecora, *Dynamic Light Scattering: With Applications to Chemistry, Biology, and Physics* (Dover, New York, 2010).
- [7] B. Alberts, R. Heald, A. Johnson, D. Morgan, M. C. Raff, K. Roberts, and P. Walter, *Molecular biology of the cell* (W. W. Norton & Company, 2022).
- [8] D. G. Cahill, W. K. Ford, K. E. Goodson, G. D. Mahan, A. Majumdar, H. J. Maris, R. Merlin, and S. R. Phillpot, Nanoscale thermal transport, *Journal of Applied Physics* **93**, 793 (2003).
- [9] J. A. Johnson, A. A. Maznev, J. Cuffe, J. K. Eliason, A. J. Minnich, T. Kehoe, C. M. Torres, G. Chen, and K. A. Nelson, Direct measurement of room-temperature nondiffusive thermal transport over micron distances in a silicon membrane, *Physical Review Letters* **110**, 025901 (2013).
- [10] R. B. Wilson and D. G. Cahill, Anisotropic failure of Fourier theory in time-domain thermoreflectance experiments, *Nature Communications* **5**, 1 (2014).
- [11] K. Zheng, S. Ghosh, and S. Granick, Exceptions to Fourier's law at the macroscale, *Proceedings of the National Academy of Sciences of the United States of America* **121**, e2320337121 (2024).
- [12] A. A. Maznev, J. A. Johnson, and K. A. Nelson, Onset of nondiffusive phonon transport in transient thermal grating decay, *Physical Review B* **84**, 195206 (2011).
- [13] J. P. Feser and D. G. Cahill, Probing anisotropic heat transport using time-domain thermoreflectance with offset laser spots, *Review of Scientific Instruments* **83**, 104901 (2012).
- [14] D. G. Cahill, P. V. Braun, G. Chen, D. R. Clarke, S. Fan, K. E. Goodson, P. Keblinski, W. P. King, G. D. Mahan, A. Majumdar, H. J. Maris, S. R. Phillpot, E. Pop, and L. Shi, Nanoscale thermal transport. II. 2003-2012, *Applied Physics Reviews* **1**, 011305 (2014).
- [15] A. J. Minnich, Advances in the measurement and computation of thermal phonon transport properties, *Journal of Physics Condensed Matter* **27**, 053202 (2015).
- [16] C. Cattaneo, Sulla conduzione del calore, *Atti Sem. Mat. Fis. Univ. Modena* **3**, 83 (1948).
- [17] M. P. Vernotte, La véritable équation de la chaleur, *Comptes Rendus Hebdomadaires Des Séances L'academie Des Sciences* **247**, 2103 (1958).
- [18] S. R. de Groot and P. Mazur, *Non-Equilibrium Thermodynamics* (Dover, New York, 1984).
- [19] J. M. Vilar and J. M. Rubí, Thermodynamics "beyond" local equilibrium., *Proceedings of the National Academy of Sciences of the United States of America* **98**, 11081 (2001).
- [20] D. Reguera, J. M. Rubí, and J. M. Vilar, The mesoscopic dynamics of thermodynamic systems, *Journal of Physical Chemistry B* **109**, 21502 (2005).
- [21] H. Mori, Transport, collective motion, and Brownian motion, *Progress of Theoretical Physics* **33**, 423 (1965).
- [22] K. Ryogo, Statistical-Mechanical Theory of Irreversible Processes. I. General Theory and Simple Applications to Magnetic and Conduction Problems, *Journal of the Physical Society of Japan* **12**, 570 (1957).
- [23] R. Zwanzig, Memory effects in irreversible thermodynamics, *Physical Review* **124**, 983 (1961).
- [24] R. Zwanzig, *Nonequilibrium statistical mechanics* (Oxford University Press, New York, 2001).
- [25] B. H. Armstrong, Two-fluid theory of thermal conductivity of dielectric crystals, *Physical Review B* **23**, 883 (1981).
- [26] L. Zhu, A. Fiorino, D. Thompson, R. Mittapally, E. Meyhofer, and P. Reddy, Near-field photonic cooling through control of the chemical potential of photons, *Nature* **566**, 239 (2019).
- [27] K. Chen and S. Fan, Nonequilibrium Casimir Force with a Nonzero Chemical Potential for Photons, *Physical Review Letters* **117**, 267401 (2016).
- [28] Supplemental Material.
- [29] K. Schwab, E. A. Henriksen, J. M. Worlock, and M. L. Roukes, Measurement of the quantum of thermal conductance, *Nature* **404**, 974 (2000).
- [30] R. Morgado, F. A. Oliveira, G. G. Batrouni, and A. Hansen, Relation between Anomalous and Normal Diffusion in Systems with Memory, *Physical Review Letters* **89**, 100601 (2002).
- [31] L. C. Lapas, I. V. L. Costa, M. H. Vainstein, and F. a. Oliveira, Entropy, non-ergodicity and non-Gaussian behaviour in ballistic transport, *Europhysics Letters (EPL)* **77**, 37004 (2007).
- [32] M. Vainstein and I. Costa, Non-exponential relaxation for anomalous diffusion, *Europhysics Letters (EPL)* **73**, 726 (2006).
- [33] L. C. Lapas, R. Morgado, M. H. Vainstein, J. M. Rubí, and F. A. Oliveira, Khinchin Theorem and Anomalous Diffusion, *Physical Review Letters* **101**, 230602 (2008).
- [34] E. G. Flekkøy, A. Hansen, and B. Baldelli, Hyperballistic Superdiffusion and Explosive Solutions to the Non-Linear Diffusion Equation, *Frontiers in Physics* **9**, 640560 (2021).
- [35] R. A. Guyer and J. A. Krumhansl, Thermal Conductivity, Second Sound, and Phonon Hydrodynamic Phenomena in Nonmetallic Crystals, *Physical Review* **148**, 778 (1966).
- [36] G. D. Mahan and F. Claro, Nonlocal theory of thermal conductivity, *Physical Review B* **38**, 1963 (1988).
- [37] C. Hua and A. J. Minnich, Analytical Green's function of the multidimensional frequency-dependent phonon Boltzmann equation, *Physical Review B* **90**, 214306 (2014).
- [38] B. Vermeersch, J. Carrete, N. Mingo, and A. Shakouri, Superdiffusive heat conduction in semiconductor alloys. I. Theoretical foundations, *Physical Review B* **91**, 085202 (2015).
- [39] Y. K. Koh and D. G. Cahill, Frequency dependence of the thermal conductivity of semiconductor alloys, *Physical Review B - Condensed Matter and Materials Physics* **76**, 075207 (2007).
- [40] M. S. Gomes-Filho, L. C. Lapas, E. Gudowska-Nowak, and F. A. Oliveira, The fluctuation-dissipation relations: Growth, diffusion, and beyond, *Physics Reports* **1141**, 1 (2025).

# Supplemental Material for “Generalized Fourier’s law in mesoscopic systems”

Luciano C. Lapas<sup>✉\*</sup>

*Latin American Institute of Life and Natural Sciences,  
Universidade Federal da Integração Latino-Americana, Av. Tancredo Neves,  
6731, Bloco 6, Espaço 3, Sala 5, Foz do Iguaçu, 85867-970, PR, Brazil.*

This Supplemental Material provides the derivations summarized in the main text. Section SI obtains the nonlocal constitutive relation [Eq. (2) of the Letter] from entropy production and linear response, and establishes its positive semidefinite (second-law) character. Section SII traces the kernel to phase-space correlations within mesoscopic nonequilibrium thermodynamics (MNET). Section SIII derives the generalized Langevin equation (GLE) [Eq. (4)] by Mori–Kubo–Zwanzig projection. Section SIV performs the modal decomposition leading to the closed-form, tensorial Onsager kernel [Eq. (6)] and its quantum (Bose) weighting [Eq. (7)]. Section SV classifies the transport regimes from the low-frequency memory spectrum. Section SVI collects technical notes on anisotropy, spatial-wavevector nonlocality, and the interface connection.

## SI HYDRODYNAMIC DERIVATION AND SECOND LAW

At the hydrodynamic level the total entropy is the volume integral of the local entropy density  $s(\mathbf{r}, t)$  [1],

$$S(t) = \int d\mathbf{r} s(\mathbf{r}, t), \quad \frac{dS}{dt} = \int d\mathbf{r} \sigma(\mathbf{r}, t) \geq 0, \quad (\text{S1})$$

where  $\sigma$  is the local production rate. For heat transport in a single-component rigid medium (no mass flow), the entropy balance gives the bilinear form  $\sigma(\mathbf{r}, t) = \mathbf{J}_q(\mathbf{r}, t) \cdot \mathbf{X}_q(\mathbf{r}, t) \geq 0$ , identifying the conjugate force

$$\mathbf{X}_q(\mathbf{r}, t) \equiv \nabla \left[ \frac{1}{T(\mathbf{r}, t)} \right]. \quad (\text{S2})$$

For small deviations from equilibrium the flux is a linear functional of the force history [2, 3]. The most general causal, time-translation-invariant linear law is

$$\mathbf{J}_q(\mathbf{r}, t) = \int_{-\infty}^t dt' \int d\mathbf{r}' \mathbf{L}_{qq}(\mathbf{r}, \mathbf{r}', t - t') \mathbf{X}_q(\mathbf{r}', t'), \quad (\text{S3})$$

with  $\mathbf{L}_{qq} = \mathbf{\Lambda}_{qq} \Theta(t - t')$  and  $\Theta$  the Heaviside function. Equation (S3) is Eq. (2) of the Letter. Inserting it into Eq. (S1) yields the quadratic functional

$$\frac{dS}{dt} = \int_{-\infty}^t dt' \iint d\mathbf{r} d\mathbf{r}' \mathbf{X}_q(\mathbf{r}, t) \cdot \mathbf{L}_{qq}(\mathbf{r}, \mathbf{r}', t - t') \cdot \mathbf{X}_q(\mathbf{r}', t'), \quad (\text{S4})$$

which must be nonnegative for arbitrary small histories of  $\mathbf{X}_q$ . This implies that the symmetric part of  $\mathbf{L}_{qq}$  defines a positive semidefinite operator (generalized Onsager positivity condition for memory kernels). For stationary kernels it is convenient to state this condition in the Fourier/Laplace domain: the dissipative (Hermitian) part of  $\tilde{\mathbf{L}}_{qq}(\mathbf{k}, \omega)$  must be positive semidefinite, i.e.  $\text{Re} \tilde{\mathbf{L}}_{qq}(\mathbf{k}, \omega) \succeq 0$  for all  $\mathbf{k}$  and real  $\omega$ .

## SII MESOSCOPIC ORIGIN OF THE KERNEL

Within MNET [4, 5], thermal transport is the stochastic evolution of carriers (phonons, photons, quasiparticles) over a phase-space landscape  $\mathbf{\Gamma} = (\mathbf{p}, \mathbf{r})$  with density  $\rho(\mathbf{\Gamma}, t)$ . The Gibbs entropy postulate  $S = -k_B \int \rho \ln(\rho/\rho_{\text{leq}}) d\mathbf{\Gamma} + S_{\text{leq}}$ , together with the phase-space continuity equation  $\partial_t \rho = -\nabla_{\mathbf{\Gamma}} \cdot \mathbf{J}$ , gives the production rate

$$\sigma = - \int \mathbf{J}(\mathbf{\Gamma}, t) \cdot \nabla_{\mathbf{\Gamma}} \left[ \frac{\mu(\mathbf{\Gamma}, t)}{T} \right] d\mathbf{\Gamma} \geq 0, \quad \mu = k_B T \ln \frac{\rho}{\rho_{\text{leq}}} + \mu_{\text{leq}}. \quad (\text{S5})$$

A causal linear law with a nonlocal phase-space kernel  $\mathbf{L}(\mathbf{\Gamma}, \mathbf{\Gamma}', t - t')$ ,

$$\mathbf{J}(\mathbf{\Gamma}, t) = \int_{-\infty}^t dt' \int d\mathbf{\Gamma}' \mathbf{L}(\mathbf{\Gamma}, \mathbf{\Gamma}', t - t') \nabla_{\mathbf{\Gamma}'} \left[ \frac{\mu(\mathbf{\Gamma}', t')}{T} \right], \quad (\text{S6})$$

recovers the standard Fokker–Planck equation in the Markovian limit  $\mathbf{L} \propto \delta(t)$ . Under local quasi-equilibrium the chemical-potential gradient is dominated by the thermal gradient,  $\nabla_{\mathbf{\Gamma}'}(\mu/T) \simeq \mathcal{A}(\mathbf{\Gamma}'; T) \nabla_{\mathbf{r}'}(1/T)$ . Coarse-graining the spatial current  $\mathbf{J}_q(\mathbf{r}, t) = \int d\mathbf{\Gamma} \varepsilon(\mathbf{\Gamma}) \mathbf{J}_{\mathbf{r}}(\mathbf{\Gamma}, t) \delta(\mathbf{r} - \mathbf{r}(\mathbf{\Gamma}))$  then reproduces Eq. (S3) with

$$\mathbf{L}_{qq}(\mathbf{r}, \mathbf{r}', \tau) = \iint d\mathbf{\Gamma} d\mathbf{\Gamma}' \varepsilon(\mathbf{\Gamma}) \mathbf{L}_{\mathbf{r}\mathbf{r}'}(\mathbf{\Gamma}, \mathbf{\Gamma}', \tau) \mathcal{A}(\mathbf{\Gamma}') \delta(\mathbf{r} - \mathbf{r}(\mathbf{\Gamma})) \delta(\mathbf{r}' - \mathbf{r}(\mathbf{\Gamma}')). \quad (\text{S7})$$

Spatial nonlocality ( $\mathbf{r} \neq \mathbf{r}'$ ) thus originates in phase-space correlations that couple distinct positions through carrier streaming and scattering.

### SIII GENERALIZED LANGEVIN EQUATION

Let  $\mathcal{L}$  be the Liouville operator,  $\dot{X} = i\mathcal{L}X$ , and let  $\mathbf{A}(\mathbf{\Gamma})$  be the column vector of relevant slow variables (energy density and heat-flux modes). The Mori–Zwanzig projector and its complement are

$$\mathcal{P}Y = \langle Y \mathbf{A}^\dagger \rangle \mathbf{C}^{-1} \mathbf{A}, \quad \mathcal{Q} = 1 - \mathcal{P}, \quad \mathbf{C} = \langle \mathbf{A} \mathbf{A}^\dagger \rangle, \quad (\text{S8})$$

with the inner product  $(X, Y) = \langle XY^\dagger \rangle_{\rho_{\text{eq}}}$ . The operator identity  $e^{it\mathcal{L}} = e^{it\mathcal{Q}\mathcal{L}} + \int_0^t d\tau e^{i(t-\tau)\mathcal{L}} i\mathcal{P}\mathcal{L} e^{i\tau\mathcal{Q}\mathcal{L}}$  applied to  $\dot{\mathbf{A}} = e^{it\mathcal{L}} i\mathcal{L} \mathbf{A}$  gives the GLE

$$\dot{\mathbf{A}}(t) = i\mathbf{\Omega} \mathbf{A}(t) - \int_0^t d\tau \mathbf{\Phi}(\tau) \mathbf{A}(t - \tau) + \mathbf{F}(t), \quad (\text{S9})$$

which is Eq. (4) of the Letter, with

$$\mathbf{\Omega} = \langle (i\mathcal{L} \mathbf{A}) \mathbf{A}^\dagger \rangle \mathbf{C}^{-1}, \quad \mathbf{F}(t) = e^{it\mathcal{Q}\mathcal{L}} \mathcal{Q}(i\mathcal{L} \mathbf{A}), \quad \mathbf{\Phi}(\tau) = \langle \mathbf{F}(\tau) \mathbf{F}^\dagger(0) \rangle \mathbf{C}^{-1}. \quad (\text{S10})$$

The last relation is the second fluctuation–dissipation theorem; the projected propagator  $e^{it\mathcal{Q}\mathcal{L}}$  keeps  $\mathbf{F}(t)$  orthogonal to  $\mathbf{A}(0)$ . For variables of equal parity,  $\mathbf{\Omega} = \mathbf{0}$  and the dynamics is purely dissipative with memory. Laplace transforming ( $\tilde{f}(z) = \int_0^\infty e^{-zt} f dt$ ),

$$\tilde{\mathbf{A}}(z) = \tilde{\mathbf{R}}(z) \mathbf{A}(0) + \tilde{\mathbf{R}}(z) \tilde{\mathbf{F}}(z), \quad \tilde{\mathbf{R}}(z) = [z\mathbf{1} + \tilde{\mathbf{\Phi}}(z)]^{-1}. \quad (\text{S11})$$

Right-multiplying by  $\mathbf{A}^\dagger(0)$  and averaging removes the noise term (orthogonality), giving  $\mathbf{C}(t) = \mathbf{R}(t) \mathbf{C}_0$  with  $\mathbf{R}(0) = \mathbf{1}$ , so that  $\mathbf{R}(t) = \mathbf{C}(t) \mathbf{C}_0^{-1}$  governs the decay of fluctuations. The decay rates are the poles of  $\tilde{\mathbf{R}}(z)$ , i.e. the roots of  $\det[z\mathbf{1} + \tilde{\mathbf{\Phi}}(z)] = 0$ .

### SIV MODAL DECOMPOSITION AND QUANTUM WEIGHTING

In a structure with dimensions comparable to the phonon MFP, the continuum spectrum is replaced by discrete eigenmodes  $\phi_\mu(\mathbf{r})$  satisfying  $\hat{\mathcal{L}}_{\text{wave}} \phi_\mu = -\omega_\mu^2 \phi_\mu$  in  $V$ , orthonormalized as  $\int_V \phi_\mu^* \phi_\nu d\mathbf{r} = \delta_{\mu\nu}$ . The harmonic energy density is  $u(\mathbf{r}, t) = \sum_\mu \varepsilon_\mu n_\mu(t) |\phi_\mu(\mathbf{r})|^2$ , and the kinetic (diagonal) heat flux is

$$\mathbf{J}_q(\mathbf{r}, t) = \sum_\mu \mathbf{\Psi}_\mu(\mathbf{r}) A_\mu(t), \quad \mathbf{\Psi}_\mu(\mathbf{r}) = \mathbf{v}_\mu(\mathbf{r}) |\phi_\mu(\mathbf{r})|^2, \quad (\text{S12})$$

with  $A_\mu(t) = \delta E_\mu(t) = \varepsilon_\mu [n_\mu(t) - n_\mu^{\text{eq}}]$  the modal energy fluctuation,  $\varepsilon_\mu = \hbar\omega_\mu$ , and  $\mathbf{v}_\mu$  the local group velocity. Taking the slow variable to be the modal energy rather than the bare population keeps the heat-capacity weighting consistent below. Inserting Eq. (S12) into the Green–Kubo definition  $L_{qq}^{ij}(\mathbf{r}, \mathbf{r}', t) = (k_B T^2)^{-1} \langle J_q^i(\mathbf{r}, t) J_q^j(\mathbf{r}', 0) \rangle$  and using  $\mathbf{C}(t) = \mathbf{R}(t) \mathbf{C}_0$  with diagonal static fluctuations  $\langle A_\mu^2 \rangle_{\text{eq}} = \langle \delta E_\mu^2 \rangle_{\text{eq}}$  gives

$$L_{qq}^{ij}(\mathbf{r}, \mathbf{r}', t) = \frac{1}{k_B T^2} \sum_{\mu, \nu} \Psi_\mu^i(\mathbf{r}) \Psi_\nu^j(\mathbf{r}') R_{\mu\nu}(t) \langle A_\nu^2 \rangle_{\text{eq}}. \quad (\text{S13})$$

For bosonic carriers the population variance is  $\langle(\delta n_\nu)^2\rangle_{\text{eq}} = n_\nu^{\text{eq}}(n_\nu^{\text{eq}} + 1)$ , so the energy variance equals  $\langle\delta E_\nu^2\rangle = (\hbar\omega_\nu)^2\langle(\delta n_\nu)^2\rangle_{\text{eq}} = k_B T^2 c_{\text{ph}}(\omega_\nu, T)$ , with

$$c_{\text{ph}}(\omega, T) = k_B \left( \frac{\hbar\omega}{2k_B T} \right)^2 \text{csch}^2 \left( \frac{\hbar\omega}{2k_B T} \right). \quad (\text{S14})$$

The prefactor  $k_B T^2$  cancels, yielding the quantum-corrected tensorial Onsager kernel [Eq. (6) of the Letter],

$$L_{qq}^{ij}(\mathbf{r}, \mathbf{r}', t) = \sum_{\mu, \nu} \Psi_\mu^i(\mathbf{r}) \Psi_\nu^j(\mathbf{r}') R_{\mu\nu}(t) c_{\text{ph}}(\omega_\nu, T). \quad (\text{S15})$$

*Second law.*—Defining projected forces  $X_\mu(t) = -T_R^{-1} \int_V d\mathbf{r} \Psi_\mu(\mathbf{r}) \cdot \nabla T(\mathbf{r}, t)$ , the entropy production [Eq. (S4)] becomes the quadratic form  $\sigma[T] = (k_B T_R^2)^{-1} \sum_{\mu, \nu} \int_{-\infty}^t dt' X_\mu(t) C_{\mu\nu}(t-t') X_\nu(t')$ . Since  $C_{\mu\nu}(t)$  is a stationary correlation matrix, the Wiener-Khinchin and Bochner theorems guarantee a non-negative-definite power spectrum, hence  $\sigma[T] \geq 0$ .

#### SIV.A Long-wavelength expansion and a minimal one-length $k$ -space form

This subsection provides a short derivation of the minimal Lorentzian wavevector dependence used in the Letter,  $\kappa_{\text{eff}}(k) = \kappa_{\text{bulk}}/[1 + (k\ell)^2]$ , as a controlled long-wavelength approximation.

*Quasistatic reduction to a spatial kernel.*—In the quasistatic regime relevant to the MHz TDTR fits in the Letter, the dominant effect is spatial nonlocality and one may consider the time-integrated (zero-frequency) kernel

$$\bar{L}_{qq}^{ij}(\mathbf{r}, \mathbf{r}') \equiv \int_0^\infty dt L_{qq}^{ij}(\mathbf{r}, \mathbf{r}', t), \quad (\text{S16})$$

and the corresponding spatial conductivity kernel  $\bar{\kappa}^{ij}(\mathbf{r}, \mathbf{r}') = \bar{L}_{qq}^{ij}(\mathbf{r}, \mathbf{r}')/T_0^2$ .

*Isotropic reduction and analyticity at  $k = 0$ .*—Assume an isotropic medium and focus on a diagonal component. Writing the spatially homogeneous kernel as an even function of the separation,

$$\bar{\kappa}(\mathbf{r}, \mathbf{r}') \equiv \bar{\kappa}(\boldsymbol{\xi}), \quad \boldsymbol{\xi} \equiv \mathbf{r} - \mathbf{r}', \quad \bar{\kappa}(\boldsymbol{\xi}) = \bar{\kappa}(-\boldsymbol{\xi}), \quad (\text{S17})$$

its spatial Fourier transform is real and analytic near  $k = 0$ :

$$\kappa(k) \equiv \int d\boldsymbol{\xi} e^{-i\mathbf{k}\cdot\boldsymbol{\xi}} \bar{\kappa}(\boldsymbol{\xi}) = \kappa(0) [1 - ak^2 + O(k^4)]. \quad (\text{S18})$$

The coefficient  $a$  is fixed by the second spatial moment of the real-space kernel. Expanding the exponential and using isotropy,

$$\begin{aligned} \kappa(k) &= \int d\boldsymbol{\xi} \bar{\kappa}(\boldsymbol{\xi}) - \frac{1}{2} \sum_{m,n} k_m k_n \int d\boldsymbol{\xi} \xi_m \xi_n \bar{\kappa}(\boldsymbol{\xi}) + O(k^4) \\ &= \kappa(0) - \frac{k^2}{2d} \int d\boldsymbol{\xi} \xi^2 \bar{\kappa}(\boldsymbol{\xi}) + O(k^4), \end{aligned} \quad (\text{S19})$$

where  $d$  is the spatial dimension. Thus,

$$a = \frac{1}{2d} \frac{\int d\boldsymbol{\xi} \xi^2 \bar{\kappa}(\boldsymbol{\xi})}{\int d\boldsymbol{\xi} \bar{\kappa}(\boldsymbol{\xi})}. \quad (\text{S20})$$

This identifies a natural nonlocal length scale,

$$\ell^2 \equiv a, \quad (\text{S21})$$

i.e.  $\ell$  is the rms range of the conductivity kernel (up to the geometric factor  $2d$ ).

*Minimal Padé resummation.*—A convenient closed form that (i) matches Eq. (S18) to order  $k^2$ , (ii) is positive and monotonically decreasing with  $k^2$ , and (iii) corresponds to a finite-range real-space kernel, is the [0/1] Padé approximant

$$\kappa(k) \simeq \frac{\kappa(0)}{1 + \ell^2 k^2}. \quad (\text{S22})$$

## SV SPECTRAL CLASSIFICATION OF TRANSPORT REGIMES

The bath spectral density fixes the memory kernel via  $\Phi(t) = (2/\pi) \int_0^\infty [\mathbf{S}(\omega)/\omega] \cos(\omega t) d\omega$ . A power law  $\mathbf{S}(\omega) \propto \omega^s$  gives  $\Phi(t) \propto t^{-s}$  and, in the Laplace domain,  $\tilde{\Phi}(z) \sim \mathbf{C}_s z^{s-1}$  ( $z \rightarrow 0$ ) [6–8]. The final-value theorem applied to  $\tilde{\mathbf{R}}(z) = [z\mathbf{1} + \tilde{\Phi}(z)]^{-1}$  gives  $\lim_{t \rightarrow \infty} \mathbf{R}(t) = \lim_{z \rightarrow 0} [\mathbf{1} + \mathbf{C}_s z^{s-2}]^{-1}$ , classifying the dynamics:

1. *Ohmic*,  $s = 1$  (*normal diffusion*).  $\tilde{\Phi}(0) = \gamma^*$  finite;  $\mathbf{R}(\infty) = \mathbf{0}$  (exponential relaxation), recovering Fourier's law and the generalized Einstein relation  $\mathbf{L}_{\text{Onsager}} = (k_B T)^{-1} [\gamma^*]^{-1} \mathbf{C}_0$ .
2. *Sub-Ohmic*,  $0 < s < 1$  (*subdiffusion*).  $\tilde{\Phi}(z) \sim z^{s-1}$  diverges; ergodic but algebraically slow relaxation,  $\alpha = s < 1$ , where  $\alpha$  is known as diffusion exponent.
3. *Super-Ohmic*,  $1 < s < 2$  (*superdiffusion*). Persistent correlations with  $\alpha > 1$ ; the system still relaxes,  $\mathbf{R}(\infty) = \mathbf{0}$ .
4. *Ballistic*,  $s = 2$ .  $\mathbf{R}(\infty) = [\mathbf{1} + \mathbf{C}_s]^{-1} \neq \mathbf{0}$ : the autocorrelation never vanishes and the hydrodynamic description breaks down [9].

Beyond  $s > 2$ , concentration-dependent diffusivity  $D(C) \sim C^{-\gamma}$  produces hyperballistic spreading that requires a nonlinear treatment [10]. The Cattaneo–Vernotte equation is recovered for a single inertial pole,  $\tilde{\Phi}(z) \approx \tau_q^{-1} \mathbf{1}$ , giving  $\tilde{\mathbf{L}}(z) = \mathbf{L}_0 / (1 + z\tau_q)$  and, in the time domain,  $\tau_q \partial_t \mathbf{J}_q + \mathbf{J}_q = -\kappa \nabla T$ . This temporal-memory limit applies when  $1/f \lesssim \tau_q$ , i.e. in second-sound and transient-grating geometries; it is *not* the regime of the quasistatic TDTR analysis below.

## SVI ANISOTROPY, WAVEVECTOR NONLOCALITY, AND THE INTERFACE

*Anisotropic conductivity.*—Fourier transforming Eq. (S15) in space and time and dividing by  $T_0^2$  gives the generalized conductivity tensor  $\kappa_{\text{eff}}^{ij}(\mathbf{k}, \omega) = \tilde{L}_{qq}^{ij}(\mathbf{k}, \omega) / T_0^2$ . Because  $\Psi_\mu$  carries the directional group velocity  $\mathbf{v}_\mu$ , the diagonal blocks are weighted by the corresponding velocity projections,

$$\kappa_{\text{eff}}^{ii}(\mathbf{k}, \omega) = \frac{1}{T_0^2} \sum_{\mu, \nu} \tilde{\Psi}_\mu^i(\mathbf{k}) \tilde{\Psi}_\nu^i(-\mathbf{k}) \tilde{R}_{\mu\nu}(\omega) c_{\text{ph}}(\omega_\nu, T), \quad (\text{S23})$$

and are in general unequal,  $\kappa_{\text{eff}}^{zz} \neq \kappa_{\text{eff}}^{rr}$ , even for a crystal whose bulk conductivity is isotropic.

In a TDTR experiment, the measured signal is, strictly, sensitive to a distribution of in-plane spatial frequencies (Hankel-space integral) [11]. It is nevertheless convenient to summarize the dominant gradients by effective wavevectors:  $k_r \sim w_0^{-1}$  (spot size) and a through-plane wavevector  $k_z \sim d_p^{-1}(f)$  associated with the oscillatory penetration depth. To avoid circularity when the apparent conductivity depends on  $f$ , we define

$$d_p(f) \equiv \sqrt{\frac{\kappa_{\text{ref}}}{\pi C f}}, \quad k_z \sim d_p^{-1}(f), \quad (\text{S24})$$

where  $\kappa_{\text{ref}}$  is a fixed diffusive reference conductivity (taken as  $\kappa_{\text{ref}} = \kappa_{\text{bulk}}$  in the numerical estimates below). Thus,

$$k_r \simeq w_0^{-1}. \quad (\text{S25})$$

The measured through- and in-plane conductivities,

$$\Lambda_z = \kappa_{\text{eff}}^{zz}(k_z), \quad \Lambda_r = \kappa_{\text{eff}}^{rr}(k_r), \quad (\text{S26})$$

differ, with the more strongly sampled direction the more suppressed. For Si at  $w_0 \approx 1 \mu\text{m}$ ,  $f = 9.8 \text{ MHz}$ ,  $\kappa_{\text{ref}} \approx 142 \text{ W m}^{-1} \text{ K}^{-1}$  and  $C \approx 1.6 \times 10^6 \text{ J m}^{-3} \text{ K}^{-1}$ , one finds  $d_p \approx 1.7 \mu\text{m}$ , hence  $k_z \approx 0.6 \mu\text{m}^{-1} < k_r \approx 1.0 \mu\text{m}^{-1}$  and  $\Lambda_r < \Lambda_z$ , consistent with the beam-offset values  $\Lambda_z \approx 140$ ,  $\Lambda_r \approx 80 \text{ W m}^{-1} \text{ K}^{-1}$  [11, 12].

*Spatial-nonlocality reduction.*—A minimal, one-length parametrization consistent with the long-wavelength expansion in Sec. SIV.A is

$$\kappa_{\text{eff}}(k) = \frac{\kappa_{\text{bulk}}}{1 + (k\ell)^2}, \quad (\text{S27})$$

with  $\ell$  the nonlocality range (an effective MFP-like length). Evaluating at  $k = k_z \sim d_p^{-1}(f)$  with Eq. (S24) yields the frequency-resolved apparent conductivity

$$\Lambda_A(f) = \frac{\kappa_{\text{bulk}}}{1 + f/f^*}, \quad f^* = \frac{\kappa_{\text{ref}}}{\pi C \ell^2}. \quad (\text{S28})$$

This is the two-parameter model ( $\kappa_{\text{bulk}}, \ell$ ) fitted in the Letter against the frequency-dependent TDTR apparent conductivities of Wilson and Cahill [12] (for their concentric-beam data at  $w_0 = 10 \mu\text{m}$ ). The crossover  $f^*$  scales as  $\ell^{-2}$ : materials with short  $\ell$  (e.g. pure Si, Si:B) stay flat across the band, while Ge and the SiGe alloys lower  $f^*$  into the measurement window and roll off.

Using digitized data of Ref. [12], representative fits yield  $\ell = 0.41 \pm 0.08$  (Ge),  $0.34 \pm 0.07$  ( $\text{Si}_{0.99}\text{Ge}_{0.01}$ ) and  $0.25 \pm 0.03 \mu\text{m}$  ( $\text{Si}_{0.2}\text{Ge}_{0.8}$ ), with  $\chi^2_\nu < 1$ ; Si and Si:B are flat and leave  $\ell$  unresolved. Two trends are consistent with Eq. (S15):  $\ell$  decreases as Ge is alloyed into Si (mass-disorder scattering shortens the carrier MFP [13]), while the high-frequency suppression deepens with alloying because the lower alloy conductivity shrinks  $d_p$  and increases the probed  $k_z \sim d_p^{-1}$ . Because  $\ell$  is a length, it can be compared with the conductivity accumulation function  $\alpha(L)$  [12]: the sub-micron values lie within the MFP range that dominates  $\alpha(L)$  in these crystals.

The same frequency window can often be fit by a temporal (Cattaneo) form  $\kappa_{\text{bulk}}/[1 + (2\pi f\tau)^2]$ ; the spatial interpretation is preferred not because the two fits are necessarily distinguishable over a narrow band, but because TDTR typically operates at  $1/f \gg \tau_{\text{carrier}}$ , so temporal memory is negligible and  $\ell$  is the physically meaningful parameter.

*Interfacial nonequilibrium resistance.*—Near a metal/sample boundary at  $z = 0$  the eigenmodes are reflected or transmitted, so the spatial overlap  $\Psi_\mu^i(\mathbf{r})\Psi_\nu^j(\mathbf{r}')$  in Eq. (S15) is truncated within a layer of thickness  $\sim \ell$ . The off-diagonal correlations  $R_{\mu\nu}(t)$  ( $\mu \neq \nu$ ) between high- and low-wavevector sectors then fail to relax to a single local temperature within that layer, producing an excess resistance localized near the interface. This provides a microscopic mechanism consistent with the interfacial nonequilibrium thermal resistance inferred from the frequency dependence of the apparent interface conductance of SiGe alloys [12]: as  $f$  increases and  $d_p$  shrinks, the measurement weights the near-interface region more heavily, transferring part of the nonequilibrium resistance from the apparent interface conductance to the apparent conductivity. The modal kernel therefore unifies the diffusive reservoir and the nonlocal ballistic channel of the two-fluid description [14, 15] within a single entropy-producing object.

---

\* luciano.lapas@unila.edu.br

- [1] S. R. de Groot and P. Mazur, *Non-Equilibrium Thermodynamics* (Dover, New York, 1984).
- [2] L. Onsager, Reciprocal Relations in Irreversible Processes. I., *Phys. Rev.* **37**, 405 (1931).
- [3] L. Onsager, Reciprocal Relations in Irreversible Processes. II., *Phys. Rev.* **38**, 2265 (1931).
- [4] J. M. Vilar and J. M. Rubi, Thermodynamics "beyond" local equilibrium., *Proceedings of the National Academy of Sciences of the United States of America* **98**, 11081 (2001).
- [5] D. Reguera, J. M. Rubí, and J. M. Vilar, The mesoscopic dynamics of thermodynamic systems, *Journal of Physical Chemistry B* **109**, 21502 (2005).
- [6] R. Morgado, F. A. Oliveira, G. G. Batrouni, and A. Hansen, Relation between Anomalous and Normal Diffusion in Systems with Memory, *Physical Review Letters* **89**, 100601 (2002).
- [7] L. C. Lapas, I. V. L. Costa, M. H. Vainstein, and F. a. Oliveira, Entropy, non-ergodicity and non-Gaussian behaviour in ballistic transport, *Europhysics Letters (EPL)* **77**, 37004 (2007).
- [8] M. Vainstein and I. Costa, Non-exponential relaxation for anomalous diffusion, *Europhysics Letters (EPL)* **73**, 726 (2006).
- [9] L. C. Lapas, R. Morgado, M. H. Vainstein, J. M. Rubí, and F. A. Oliveira, Khinchin Theorem and Anomalous Diffusion, *Physical Review Letters* **101**, 230602 (2008).
- [10] E. G. Flekkøy, A. Hansen, and B. Baldelli, Hyperballistic Superdiffusion and Explosive Solutions to the Non-Linear Diffusion Equation, *Frontiers in Physics* **9**, 640560 (2021).
- [11] J. P. Feser and D. G. Cahill, Probing anisotropic heat transport using time-domain thermoreflectance with offset laser spots, *Review of Scientific Instruments* **83**, 104901 (2012).
- [12] R. B. Wilson and D. G. Cahill, Anisotropic failure of Fourier theory in time-domain thermoreflectance experiments, *Nature Communications* **5**, 1 (2014).
- [13] Y. K. Koh and D. G. Cahill, Frequency dependence of the thermal conductivity of semiconductor alloys, *Physical Review B - Condensed Matter and Materials Physics* **76**, 075207 (2007).
- [14] B. H. Armstrong, Two-fluid theory of thermal conductivity of dielectric crystals, *Physical Review B* **23**, 883 (1981).
- [15] A. A. Maznev, J. A. Johnson, and K. A. Nelson, Onset of nondiffusive phonon transport in transient thermal grating decay, *Physical Review B* **84**, 195206 (2011).